JOURNAL OF THEORETICAL
AND APPLIED MECHANICS
63, 3, pp. 551–556, Warsaw 2025
https://doi.org/10.15632/jtam-pl/202764

DIGITAL IMAGE CORRELATION IN MONITORING OF FATIGUE DAMAGE DEVELOPMENT OF MAR-M247 WITH ALUMINIDE COATING

Mateusz KOPEC

Institute of Fundamental Technological Research, Polish Academy of Sciences, Warsaw, Poland
mkopec@ippt.pan.pl

This study investigates the fatigue damage development in MAR-M247, a nickel-based superalloy with aluminide coating, using the digital image correlation (DIC) technique. The alloy's microstructures, including fine, coarse, and columnar grains, were analyzed to understand their influence on fatigue crack initiation and propagation. Fatigue tests were conducted at room temperature under controlled force, with strain evolution monitored through non-contact full-field DIC measurements. Results revealed that fine-grained MAR-M247 exhibited superior fatigue resistance due to uniform strain distribution, while coarse-grained and columnar structures showed pronounced strain localization and earlier crack initiation. The application of aluminide coatings did not significantly affect strain distribution across the different microstructures but highlighted complex interactions between coating and grain structure under cyclic loading. These findings provide critical insights into optimizing the performance of MAR-M247 for high-stress applications.

Keywords: fatigue; coatings; nickel alloys; digital image correlation.

1. Introduction

Nickel-based superalloys such as MAR-M247 are extensively used in high-performance applications, including gas turbine blades and aerospace components, due to their exceptional strength, thermal stability, and resistance to oxidation and corrosion at elevated temperatures (Kukla *et al.*, 2020). The complex, precipitation-strengthened microstructure of MAR-M247 is designed to maintain mechanical integrity under extreme conditions. However, the alloy's susceptibility to fatigue damage, especially under cyclic loading conditions, necessitates advanced techniques to monitor and predict failure mechanisms. One should highlight that the fatigue behavior of MAR-M247 is complex and highly dependent on temperature, stress conditions, and microstructural characteristics. At room temperature and intermediate temperatures, fatigue failure is typically dominated by crack initiation at microstructural defects such as casting pores, carbide particles, or inclusions (Kopec, 2023). These defects act as stress concentrators, leading to early crack formation. The propagation of fatigue cracks in this regime is mostly transgranular, following crystallographic slip planes due to the alloy's high strength and resistance to grain boundary sliding. At high temperatures (above 800 °C), fatigue behavior becomes

Ministry of Science and Higher Education
Republic of Poland

The publication has been funded by the Polish Ministry of Science and Higher Education under the Excellent Science II programme "Support for scientific conferences".
The content of this article was presented during the 40th Danubia-Adria Symposium on Advances in Experimental Mechanics, Gdańsk, Poland, September 24–27, 2024.

more influenced by environmental factors, particularly oxidation and creep (Šulák *et al.*, 2016). Oxidation-assisted fatigue leads to the formation of oxide layers along the crack path, which can accelerate crack growth by embrittling the surrounding material and reducing the effective load-bearing cross-section. Additionally, creep-fatigue interaction plays a crucial role, where sustained loads during cyclic loading allow time-dependent plastic deformation (creep) to contribute to crack growth, often leading to intergranular fracture as grain boundaries become weaker due to oxidation and the formation voids (Kopec, 2024a).

Digital image correlation (DIC) has emerged as a powerful tool for monitoring fatigue damage in metallic materials. By providing full-field, non-contact strain measurements, DIC enables precise tracking of strain localization, crack initiation, and propagation under various loading conditions. When applied to MAR-M247, DIC offers insights into how its microstructural characteristics influence fatigue behavior, particularly in the presence of protective aluminide coatings.

The microstructure of MAR-M247 can be tailored into fine-grained, coarse-grained, or columnar configurations, each offering distinct mechanical properties (Garimella *et al.*, 1997). Fine-grained structures are generally isotropic and exhibit improved resistance to crack initiation due to grain boundary strengthening. Coarse-grained structures, with larger grains, tend to concentrate strain at grain boundaries, making them prone to early crack initiation. Columnar structures, characterized by elongated grains aligned along the solidification direction, introduce significant anisotropy, affecting strain localization and fatigue performance. The addition of aluminide coatings further complicates this behavior. These coatings provide enhanced resistance to oxidation and hot corrosion but can introduce residual stresses and modify surface strain distributions (Kopec, 2024b). Investigating how these coatings interact with different microstructures during fatigue loading is critical to optimizing MAR-M247's performance in service.

This study employs DIC to examine the strain distribution and localization in fine-grained, coarse-grained, and columnar MAR-M247 during fatigue. Emphasis is placed on understanding how microstructural features influence fatigue crack initiation and propagation, as well as the role of aluminide coatings in altering strain evolution and fatigue life. By correlating DIC results with microstructural observations, this work aims to provide deeper insights into the complex interplay between material microstructure, surface coatings, and fatigue damage mechanisms.

2. Materials and methods

The initial microstructure of MAR-M247 of chemical composition presented in Table 1 varies based on casting conditions, producing fine, coarse, or columnar structures of the average grain size around 0.5 mm, 2.5 mm, and 5 mm, respectively (Fig. 1). In fine-grained forms, rapid cooling yields small, equiaxed grains with uniformly distributed gamma γ matrix and γ' precipitates (Fig. 1a), enhancing moderate-temperature strength and fatigue resistance. Coarse-grained structures, formed through slower cooling, feature larger grains (Fig. 1b) with an uneven precipitate distribution, improving high-temperature creep resistance but reducing fatigue performance. Columnar structures (Fig. 1c), common in directional solidification processes, exhibit elongated grains aligned along the growth direction, optimising creep and thermal fatigue properties in turbine blades due to reduced grain boundary sliding. Carbides and borides are present in all structures, influencing mechanical stability and crack resistance. Subsequently, aluminide coatings were applied through the Chemical Vapor Deposition (CVD) process with the optimized parameters (Kukla *et al.*, 2020) presented in Table 2.

Table 1. Chemical composition of MAR-M247 nickel based superalloy [wt.%].

C	Cr	Mn	Si	W	Co	Al	Ni
0.09	8.80	0.10	0.25	9.70	9.50	5.70	bal.

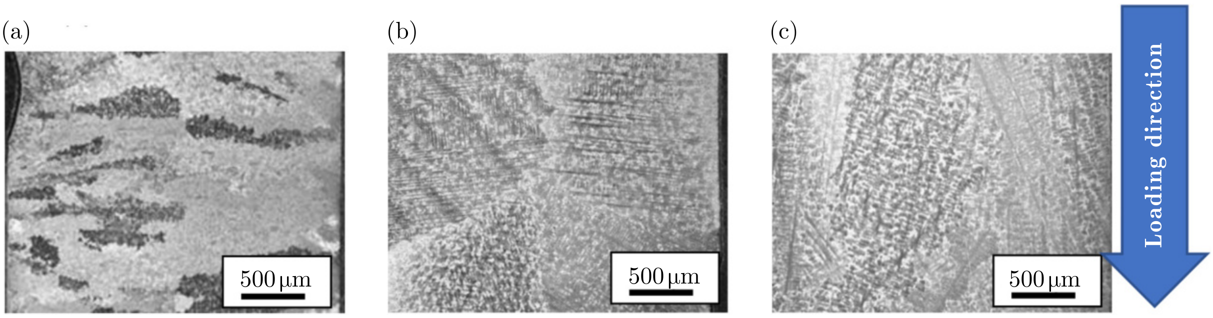

Fig. 1. Initial microstructures of MAR-M247: (a) fine; (b) coarse; (c) column-grained.

Table 2. CVD process parameters (Kukla *et al.*, 2020).

Deposition temperature	Internal pressure	Protective atmosphere	Deposition time	Coating thickness
1040 °C	150 mbar	hydrogen	8 hours	20 µm

Fatigue testing was conducted using the MTS 810 testing system (MTS System, Minnesota, USA) equipped with a standard MTS extensometer on specimens presented in Fig. 2. Uniaxial tensile evaluations were performed at a strain rate of $2 \times 10^{-4}\,\mathrm{s}^{-1}$ using five specimens. Fatigue assessments at room temperature (23 °C) were force-controlled with zero mean load, constant stress amplitude, and a frequency of 20 Hz. Each test was repeated at least twice to ensure consistent and reliable results. The stress amplitude range of 350 MPa to 650 MPa was determined based on the conventional yield strength derived from the tensile test. The strain evolution was monitored using DIC Aramis 12M setup.

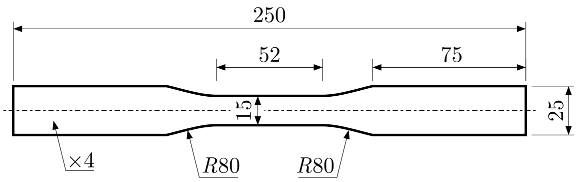

Fig. 2. Engineering drawing of coated MAR-M247 specimen for mechanical testing.

3. Results and discussion

The stress-strain curves for investigated MAR-M247 were presented in Fig. 3a. It was found, that all initial microstructures are characterized by similar yield strength of about 820 MPa, while

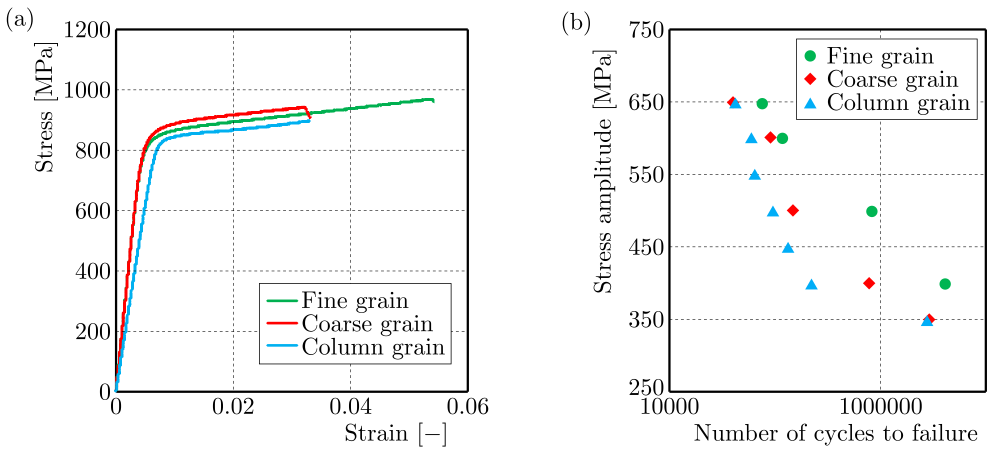

Fig. 3. Tensile (a) and fatigue (b) response of MAR-M247 alloy with three different initial microstructures and coating thickness of 20 µm.

the ultimate tensile strength and elongation are slightly higher for the fine grain. Subsequent fatigue testing revealed significantly improved response of fine-grained MAR-M247 reflected by the increased number of cycles to failure (Fig. 3b). The analysis of fatigue behavior at stress amplitude of 600 MPa using DIC revealed distinct strain distribution patterns associated with the alloy's initial microstructures (Fig. 4). Each microstructure displayed unique strain evolution

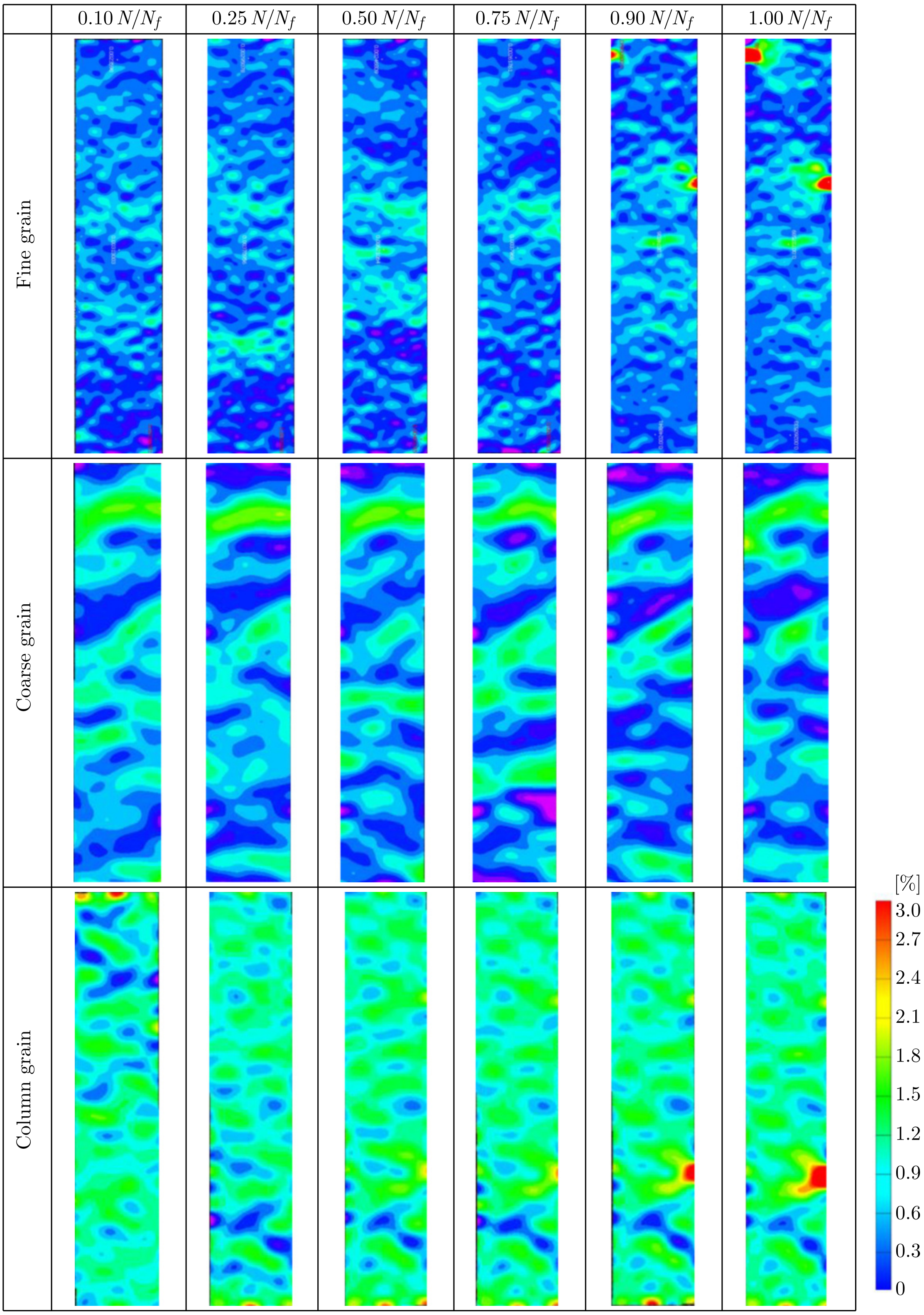

Fig. 4. Strain distribution in aluminized MAR-M247 subjected to stress amplitude of 600 MPa.

characteristics that significantly influenced fatigue crack initiation and propagation, underscoring the critical role of microstructure in determining the alloy's mechanical performance (Šulák & Obrtlík, 2025). Fine-grained MAR-M247 exhibited the most uniform strain distribution among the studied microstructures. DIC images showed minimal strain localization at early stages of cyclic loading. This behavior is attributed to the high density of grain boundaries in fine-grained structures, which act as barriers to dislocation motion, effectively distributing strain throughout the material. During fatigue loading, the delayed onset of localized strain bands and the lower severity of strain gradients contributed to prolonged resistance to crack initiation. These findings highlight the advantages of fine-grained MAR-M247 in applications where fatigue resistance is a priority. In coarse-grained MAR-M247, DIC captured pronounced strain localization more likely at grain boundaries. The larger grain size reduces the number of boundaries, concentrating strain in fewer locations and promoting early crack initiation. Strain maps revealed sharp gradients and isolated hotspots, corresponding to regions of microstructural discontinuity. These results align with the known anisotropic behavior of coarse-grained materials, where strain accumulation is less uniformly distributed, making them more susceptible to fatigue damage (Garimella *et al.*, 1997). The columnar microstructure presented a highly isotropic strain distribution, as observed in the DIC strain maps. Strain localization was strongly oriented along the grain aligned with the columnar grain growth direction which was also pararel to loading direction. One should highlight, however, that the application of aluminide coatings do not influence strain distribution across all microstructures as the strain areas represents directly grain interaction during cyclic loading.

The plastic strain accumulation capacity for each MAR-M247 microstructure significantly influences its fatigue life, as observed by the DIC analysis. Fine-grained MAR-M247 exhibited the highest plastic strain accumulation capacity due to its numerous grain boundaries, which effectively distributed strain and delayed localized deformation, resulting in superior fatigue resistance. Coarse-grained structures, with fewer grain boundaries, showed more pronounced strain localization, particularly at grain boundaries, leading to early crack initiation and reduced fatigue life. The columnar microstructure displayed anisotropic strain distribution, with strain localization aligning along the columnar grain growth direction, influencing fatigue performance depending on the loading orientation. The aluminide coatings did not significantly alter strain distribution across the different microstructures, indicating that the grain structure remains the dominant factor in fatigue behavior. Overall, fine-grained MAR-M247 demonstrated the best fatigue resistance due to its ability to accommodate plastic strain more uniformly, while coarse and columnar structures were more prone to early fatigue failure due to localized strain accumulation. A material with higher plastic strain accumulation capacity often has a lower service life because excessive plastic deformation accelerates fatigue damage mechanisms (Paul, 2025). Repeated plastic straining leads to localized stress concentrations, promoting early crack initiation at microstructural defects like grain boundaries and inclusions. Once cracks form, they propagate faster under cyclic loading, reducing fatigue life. Additionally, materials with high plastic strain tend to experience softening due to dislocation motion, making them more susceptible to failure (Paul, 2025). In high-temperature environments, accumulated strain also contributes to creep-fatigue interactions and oxidation-assisted crack growth, further diminishing durability. While beneficial in monotonic loading, excessive plastic strain in fatigue conditions accelerates microstructural deterioration, ultimately shortening service life.

4. Conclusions

The DIC data demonstrated that initial microstructure plays a critical role in determining strain evolution and fatigue behavior in MAR-M247. Fine-grained structures exhibited superior fatigue resistance due to their ability to distribute strain uniformly, while coarse-grained and columnar structures showed greater strain localization, leading to earlier crack initiation. The interaction of aluminide coatings with these microstructures introduced complex strain redistribution patterns, which require careful consideration when designing components and applying coatings.

Acknowledgments

The author would like to express his gratitude to the technical staff – M. Wyszkowski and A. Chojnacki for their kind help during the experimental part of this work. The methodological support of Prof. D. Kukla is also acknowledged.

References

1. Garimella, L., Liaw, P.K., & Klarstrom, D.L. (1997). Fatigue behavior in nickel-based superalloys: A literature review. *JOM*, *49*(7), 67–71. https://doi.org/10.1007/BF02914771
2. Kopec, M. (2023). Fatigue damage development in 14MoV6-3 steel for power plant pipes monitored by Digital Image Correlation. *Acta Mechanica Solida Sinica*, *36*(3), 405–417. https://doi.org/10.1007/s10338-023-00387-y
3. Kopec, M. (2024a). Effect of aluminide coating thickness on high-temperature fatigue response of MAR-M247 nickel-based superalloy. *Coatings*, *14*(8), Article 1072. https://doi.org/10.3390/coatings14081072
4. Kopec, M. (2024b). Recent advances in the deposition of aluminide coatings on nickel-based superalloys: A synthetic review (2019–2023). *Coatings*, *14*(5), Article 630. https://doi.org/10.3390/coatings14050630
5. Kukla, D., Kopec, M., Kowalewski, Z.L., Politis, D.J., Jóźwiak, S., & Senderowski, C. (2020). Thermal barrier stability and wear behavior of CVD deposited aluminide coatings for MAR 247 nickel superalloy. *Materials*, *13*(17), Article 3863. https://doi.org/10.3390/ma13173863
6. Kukla, D., Kopec, M., Wang, K., Senderowski, C., & Kowalewski, Z.L. (2021). Nondestructive methodology for identification of local discontinuities in aluminide layer-coated MAR 247 during its fatigue performance. *Materials*, *14*(14), Article 3824. https://doi.org/10.3390/ma14143824
7. Paul, S.K. (2025). A review on cyclic hardening and softening behavior of alloys. *Journal of Alloys and Metallurgical Systems*, *9*, Article 100153. https://doi.org/10.1016/j.jalmes.2025.100153
8. Šulák, I., & Obrtlík, K. (2025). Assessment of dwell-fatigue properties of nickel-based superalloy coated with a multi-layered thermal and environmental barrier coating. *International Journal of Fatigue*, *191*, Article 108693. https://doi.org/10.1016/j.ijfatigue.2024.108693
9. Šulák, I., Obrtlík, K., & Čelko, L. (2016). High-temperature low-cycle fatigue behaviour of HIP treated and untreated superalloy MAR-M247. *Kovove Materiály – Metallic Materials*, *54*(6), 471–481. https://doi.org/10.4149/km_2016_6_471

Manuscript received January 23, 2024; accepted for publication March 8, 2025; published online July 2, 2025.